The role of interface disorder in the thermal boundary conductivity between two crystals

1991 J. Phys.: Condens. Matter 3 1443

(http://iopscience.iop.org/0953-8984/3/11/006)

J. Phys.: Condens. Matter 3 (1991) 1443–1452. Printed in the UK

The role of interface disorder in the thermal boundary conductivity between two crystals

D Kechrakos
University of Exeter, Department of Physics, Stocker Road, Exeter EX4 4QL, UK

Received 28 August 1990

Abstract. The Kapitza conductivity (thermal boundary conductivity (TBC)) between two crystals is studied within a simple three-dimensional lattice dynamical model and the role of interface roughness on an atomic scale is investigated. The interface roughness is modelled by a random alloy monolayer $A_{1-x}B_x$ between the two semi-infinite crystals A and B and is treated by bulk alloy techniques adopted to the interface geometry. The dependence of the TBC on the acoustic mismatch between the two crystals and the degree of roughness is shown for a variety of parameter values. Our results indicate in all cases an *increase* in the TBC with respect to the planar boundary; the increase becomes quite substantial (about 300%) for large acoustic mismatch values (about $\frac{1}{3}$) and is due to diffuse phonon scattering. A comparison with two limiting models that assume only specular or completely diffuse scattering is made.

1. Introduction

The determination of the heat flux crossing the boundary between two media, when at least one of them is an insulator, and the associated phonon boundary scattering mechanism, are presently not fully understood [1]. Discrepancies between theory and experiments have been reported for solid–liquid He and solid–solid interfaces, while diffuse phonon boundary scattering has been recognized as the mechanism mainly responsible for these discrepancies.

In the case of solid–solid boundaries, which will concern us here, recent progress in the field is characterized by two achievements: first, the growth of high quality heterojunctions by, for example, molecular beam epitaxy (MBE) and related techniques and, second, the dominant participation of high-frequency phonons in the heat transfer process; the high-frequency (about 1 THz) phonons are either generated by heat pulse techniques [2] or excited in room-temperature conductivity measurements [3–6]. These experiments motivated theoretical calculations of the phonon boundary cross section and the associated thermal boundary conductivity (TBC) in the framework of lattice dynamics theory [7–11] as opposed to earlier studies within elasticity theory. The dispersion effects were shown to decrease the phonon transmission coefficient [7, 9–11] and consequently the TBC [7]. The possibility of polarization mixing (mode conversion) at the boundary has been demonstrated for a linear chain model [9] and a 3D model of the Ge–GeAs(001) interface [10]. Finally, the first detailed model study of the TBC between two FCC lattices appeared recently [11] and the temperature dependence of the TBC was shown to be similar to that of the bulk heat capacity; the mismatch of the

0953-8984/91/111443 + 10 $03.50

vibrational densities of states (VDOS) was shown to have a strong effect on the TBC, while the interface coupling strength plays only a secondary role, as long as it varies between the two crystal limits.

However, all these calculations have been based on the assumption that the boundary is planar on an atomic scale, which is very well known to be an oversimplification of any realistic situation. Interface imperfections (roughness) are always present and scatter the incident phonons *diffusely*. Consequently, some of the incident phonons that would be totally reflected if the boundary were planar do transmit by changing the value of their parallel momentum, and the overall transport across the boundary is largely modified. With respect to conductivity experiments, the effect of diffuse scattering is expected to be more pronounced at temperatures at which the dominant phonon wavelength is comparable to the defect size. This is, for example, the case for atomic-scale defects (a few Ångströms) in the high-T regime. Experimental evidence for deviations of the high-T TBC from the predictions for a planar boundary appeared recently [3–5] and the role of interface quality as a cause of these deviations has been underlined. Many theoretical efforts have been made in the past [12] to include the diffuse scattering channel in the calculation of the TBC, but they were all restricted to the low-T regime where the dispersion effects are negligible and the solid is treated as an elastic continuum.

In a previous paper [13], we presented a lattice dynamical formalism for the calculation of the phonon boundary cross section at a microscopically rough interface between two crystals. The purpose of this paper is to use this formalism to calculate the TBC of such an interface and to discuss the role of interface roughness. Also, a comparison with two limiting models is made, namely, a model that assumes the presence of a perfectly ordered boundary layer of intermediate impedance and the diffuse mismatch model (DMM) of Swartz and Pohl [6] that assumes completely diffuse boundary scattering. To do this, we use an interface between two simple cubic lattices with first-nearest-neighbour interactions. Although our lattice model is highly simplified, mainly because it does not allow for polarization mixing at the boundary, it demonstrates clearly the effect of a thin disordered boundary layer on the TBC while it reproduces the basic features of more realistic models [10, 11]. In section 2 we give the definitions of the basic physical quantities and derive the expression of the TBC for a single-branch model. The symmetry properties of the TBC are discussed, and the microscopic and phenomenological approaches to the calculation of the transmission probability are described. In section 3 we give the numerical results for the simple-cubic interface and in the last section we summarize our findings and relate these to recent experiments.

2. Formalism

2.1. Thermal boundary conductivity

When the two sides of an interface are at temperatures T and $T - \Delta T$, there is a net heat flux $\Delta\dot{Q}(T)$ across the boundary per unit area per unit time. The TBC is then defined [6] as

$$\sigma(T) = \Delta\dot{Q}(T)/\Delta T. \tag{1}$$

The net flux $\Delta\dot{Q}(T)$ is the difference between the fluxes crossing the boundary in opposite directions:

$$\Delta\dot{Q}(T) = |\dot{Q}_{A\to B}(T)| - |\dot{Q}_{B\to A}(T-\Delta T)| \qquad \Delta T \to 0^+. \tag{2}$$

In particular, the flux from A to B is

$$\dot{Q}_{A\to B}(T) = \iiint_{3BZ}^{+} \frac{d^3k}{(2\pi)^3} n(\omega_A(k), T)\hbar\omega_A(k)v_A(k)t_{BA}(k) \tag{3}$$

where $n(\omega, T)$ is the equilibrium Bose–Einstein distribution, $v_A(k)$ the perpendicular to the boundary component of the phonon group velocity and $t_{BA}(k)$ the transmission probability for an incident phonon of wavevector k; its derivation is discussed below. The + sign at the integral means that only phonons travelling *towards* the interface contribute. Contribution from different phonon branches are neglected in equation (3), which is therefore valid within the single-branch approximation adopted in this work. A symmetric expression holds for the flux from B to A. One could perform numerically the summation in equation (3) by generating a large set of points in the bulk crystal Brillouin zone. However, this procedure is quite cumbersome even for a periodic boundary [11], as a selection rule must be implemented for the points that conserve the phonon energy (and parallel momentum, if the boundary is periodic). However, it would be quite beneficial if the scattering events are grouped according to the incident phonon frequency, which implies the following transformation:

$$\iiint_{3BZ} \frac{d^3k}{(2\pi)^3} \to \int_0^\infty \frac{d\omega}{2\pi}\frac{dq}{d\omega} \iint_{S_A(\omega)} \frac{d^2k_p}{(2\pi)^2} = \int_0^\infty \frac{d\omega}{2\pi} \frac{1}{v_A(k_p, \omega)} \iint_{S_A(\omega)} \frac{d^2k_p}{(2\pi)^2} \tag{4}$$

where k_p is the component of the phonon wavevector parallel to the boundary and q the component perpendicular to it. Note that, although the Cartesian components of k are independent variables, the new variables (ω, k_p) are not, because they are related through the phonon dispersion. For this reason, the integral over k_p in equation (4) extends only over the projection S_A of the phonon isofrequency surface on the two-dimensional Brillouin zone corresponding to the interface plane structure [13]. After this transformation, equation (3) reads

$$\dot{Q}_{A\to B}(T) = \int_0^\infty \frac{d\omega}{2\pi} n(\omega, T)\hbar\omega F_{BA}(\omega) \tag{5}$$

where

$$F_{BA}(\omega) = \iint_{S_A(\omega)} \frac{d^2k_p}{(2\pi)^2} t_{BA}(k) \equiv F(m_A, m_B; \omega) \tag{6}$$

is the transmission spectral density (TSD) [11] with dependence on the atomic masses of the two crystals indicated. The dependence on the force constants is not considered here; the validity of the mass approximation for the interface is discussed at the beginning of section 3. The following two symmetry properties hold for the TSD:

(i) the *detailed balance*

$$F(m_A, m_B; \omega) = F(m_B, m_A; \omega) \tag{7a}$$

(ii) the *scaling law*

$$F(m_A, m_B; \omega) = F(\lambda m_A, \lambda m_B; \lambda^{1/2}\omega) \qquad \lambda \in \mathbb{R}. \tag{7b}$$

Equation (7*a*) expresses the thermodynamic requirement that no net flux should

occur when the system is at equilibrium ($\Delta T = 0$), and it is a direct consequence of the reciprocity relation obeyed by the transmission coefficient [13]. Equation (7*b*) indicates that the TSD is only a function of the mass ratio $r = m_B/m_A$. As a consequence of these two equations, only interfaces with $r \leqslant 1$ (or $r \geqslant 1$) need to be studied. We would like to point out here that it is not straightforward that equation (7*a*) is valid for a diffuse boundary; however, because the diffuse scattering is calculated in a self-consistent manner [13], no dissipation enters the system and the scattering process is reversible.

The average transmission coefficient for phonons of frequency ω is defined as

$$\langle t_{BA}(\omega)\rangle = \iiint_{3BZ} \frac{d^3k}{(2\pi)^3}\,\delta(\omega-\omega_k)\nu_A(k)t_{BA}(k) \Big/ \iiint_{3BZ} \frac{d^3k}{(2\pi)^3}\,\delta(\omega-\omega_k)\nu_A(k) \tag{8}$$

and one can easily show, using equation (6), that

$$\langle t_{BA}(\omega)\rangle = [(2\pi)^2/S_A(\omega)]F_{BA}(\omega). \tag{9}$$

Finally, because of the detailed-balance condition, equation (7*a*), the TBC can be written as

$$\sigma(T) = \int_0^\infty \frac{d\omega}{2\pi}\frac{\partial n(\omega,T)}{\partial T}\hbar\omega F_{BA}(\omega) \equiv \sigma(m_A, m_B; T) \tag{10}$$

and the following symmetries hold as a consequence of equation (7):

(i) the *interchange symmetry*

$$\sigma(m_A, m_B; T) = \sigma(m_B, m_A; T) \tag{11a}$$

(ii) the *scaling law*

$$\sigma(m_A, m_B; T) = \sigma(\lambda m_A, \lambda m_B; \lambda^{1/2}T) \qquad \lambda \in \mathcal{R}. \tag{11b}$$

As mentioned above, equation (11) implies that only systems with $r \leqslant 1$ (or $r \geqslant 1$) need to be studied.

Furthermore, we denote by ω_D and T_D the Debye frequency and Debye temperature, respectively, and define the reduced frequency $\Omega = \omega/\omega_D$ and reduced temperature $\Theta = T/T_D$. Equation (10) then provides

$$\sigma(\Theta) = \frac{k_B\omega_D}{2\pi}\int_0^\infty d\Omega\, C(\Omega,\Theta)F_{BA}(\Omega)$$

$$C(\Omega,\Theta) = (x^2\exp x)(\exp x - 1)^2 \qquad x = \Omega/\Theta \tag{12}$$

where $C(\Omega,\Theta)$ is the heat capacity per phonon of frequency Ω at temperature Θ. In the limit of very high temperatures,

$$\lim_{\Theta\to\infty}[C(\Omega,\Theta)] = 1 \tag{13}$$

and the conductivity reaches a saturation value given by

$$\sigma(\infty) = \frac{k_B\omega_D}{2\pi}\int_0^\infty d\Omega\, F_{BA}(\Omega). \tag{14}$$

2.2. *Microscopic calculation of $t_{BA}(k)$*

For a boundary between two crystals that deviates from perfect crystallinity, the transmission coefficient can be written in the form

$$t_{BA}(k) = t^{sp}_{BA}(k) + t^{d}_{BA}(k) \qquad \omega = \text{fixed} \tag{15}$$

where (k, ω) characterizes the incident phonon, A and B indicate the two crystals, and

the superscripts represent the types of scattering process, namely specular or diffuse. Each term in equation (15) is a sum over all final states, consistent with the selection rules, of the squared scattering amplitudes weighted by the densities of the initial and final states. In the Green function method, used here, the scattering amplitude is the Fourier transform of the appropriate **t**-matrix; the latter can be, in turn, written as a sum of two terms describing the scattering off an effective (periodic) boundary and the fluctuations away from it [13]. In this work, we assume that the interface deviations from crystallinity are due to interdiffusion of both types of atom that form a thin interface alloy layer. The various approximations in performing the configurational average for the interface alloy [13] are included in the calculation for the transmission coefficient. In the next section, we compare the results of two approximations: the virtual crystal approximation (VCA) and the coherent potential approximation (CPA) [14]. The VCA describes the random alloy as a crystal with average mass and force constant values, and it completely neglects the alloy fluctuations which give rise to the diffuse component in equation (15). The CPA includes in a self-consistent way the single-site alloy fluctuations only.

2.3. *Phenomenological calculation of* $t_{BA}(k)$

According to the DMM [6], the interface imperfections act as spherically symmetric radiating centres that emit the incident flux into the two sides of the boundary irrespective of the incoming direction. This assumption dictates the approximation

$$t_{BA}(k) \simeq \langle t_{BA}(\omega)\rangle \tag{16}$$

and from this

$$\langle t_{AB}(\omega)\rangle = \langle r_{AA}(\omega)\rangle = 1 - \langle t_{BA}(\omega)\rangle \tag{17}$$

where r_{AA} is the reflection coefficient for side A; the first equality in equation (17) expresses the loss of 'memory' of the incident phonon as regards its origin and the second the flux conservation law. Furthermore, in thermodynamic equilibrium ($\Delta T = 0$) the fluxes in opposite directions must be equal:

$$\int_0^\infty \frac{d\omega}{2\pi} n(\omega, T)\hbar\omega\langle t_{BA}(\omega)\rangle \iint_{S_A(\omega)} \frac{d^2k_p}{(2\pi)^2} 1 = \int_0^\infty \frac{d\omega}{2\pi} n(\omega, T)\hbar\omega \times[1 - \langle t_{BA}(\omega)\rangle] \iint_{S_B(\omega)} \frac{d^2k_p}{(2\pi)^2} 1 \tag{18}$$

from which

$$S_A(\omega)\langle t_{BA}(\omega)\rangle = S_B(\omega)[1 - \langle t_{BA}(\omega)\rangle]$$

and

$$\langle t_{BA}(\omega)\rangle = S_B(\omega)/[S_A(\omega) + S_B(\omega)]. \tag{19}$$

Finally, the TSD is obtained from equation (9):

$$F_{BA} = [1/(2\pi)^2]\{S_A(\omega)S_B(\omega)/[S_A(\omega) + S_B(\omega)]\}. \tag{20}$$

3. Numerical results

Consider a (001) interface between two monoatomic lattice-matched simple-cubic crystals with first-nearest-neighbour forces. In this lattice model, the three directions of

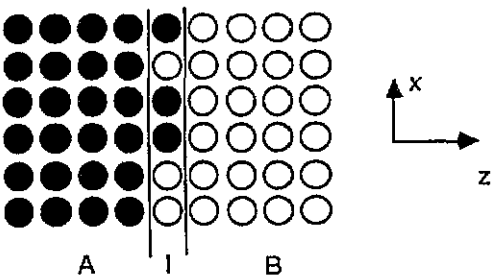

Figure 1. Microscopic model of the rough interface.

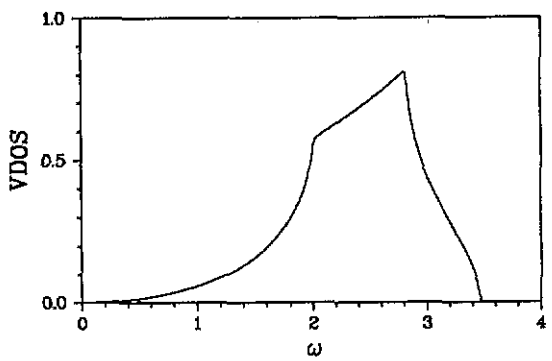

Figure 2. VDOS for the simple cubic model. Van Hove singularities occur at $\omega = 2$ and $\omega = 2^{1/2}$; the maximum frequency is $\omega_m = 12^{1/2}$.

atomic motion are completely decoupled and the calculation is therefore restricted to a single-phonon branch. The parameters of the model are the atomic mass m and the force constant f. As has been demonstrated in [11], the TBC is very sensitive to the VDOS mismatch rather than to the model parameters themselves; therefore, we can simplify the calculation by assuming that the two crystals have the same force constants and vary the mismatch through the m-values only. Furthermore, we assume that the interface roughness consists of only one atomic plane at the interface which is randomly occupied by atoms of both crystals (figure 1). The microscopic transmission coefficient for this model has been studied previously [13].

The dispersion relation of the simple-cubic crystal with first-nearest-neighbour couplings is

$$\omega^2(k) = \omega_0^2[3 - \cos(k_x a) - \cos(k_y a) - \cos(qa)]$$

where $k = (k_x, k_y, q) = (k_p, q)$, $\omega_0^2 = 2f/m$ and a is the lattice constant. The VDOS for the bulk crystal is shown in figure 2. The acoustic impedance Z is defined as the prodiuct of the sound velocity c_s and the mass density ρ. In our model, $\rho = m/a^3$, and the sound velocity is obtained from the Taylor's expansion of the dispersion relation for small wavevectors; the result is $c_s = a\omega_0$ and, therefore, $Z = a^2(2fm)^{1/2}$.

The analysis of the thermal properties that follows requires the determination of the Debye frequency ω_D. This is obtained from $\omega_D = k_D c_s$, where k_D is the Debye wavevector, which is equal to the radius of a sphere in k-space that contains the same number of states as the bulk Brillouin zone; we obtain $k_D = a(6\pi^2)^{1/3}$ and, finally, $\omega_D = (6\pi^2)^{1/3}\omega_0$.

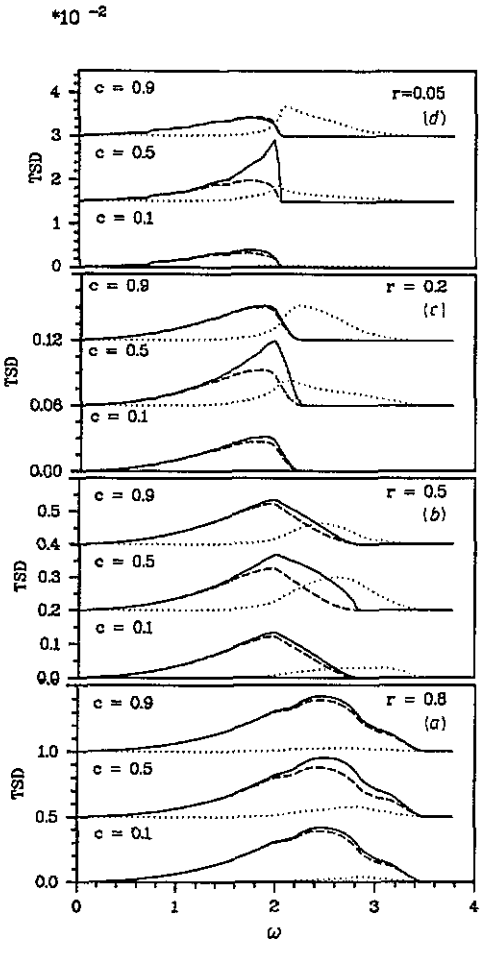

Figure 3. Comparison between CPA and VCA results for the TSD: – – –, specular component of CPA; · · · ·, diffuse component of CPA; ——, VCA.

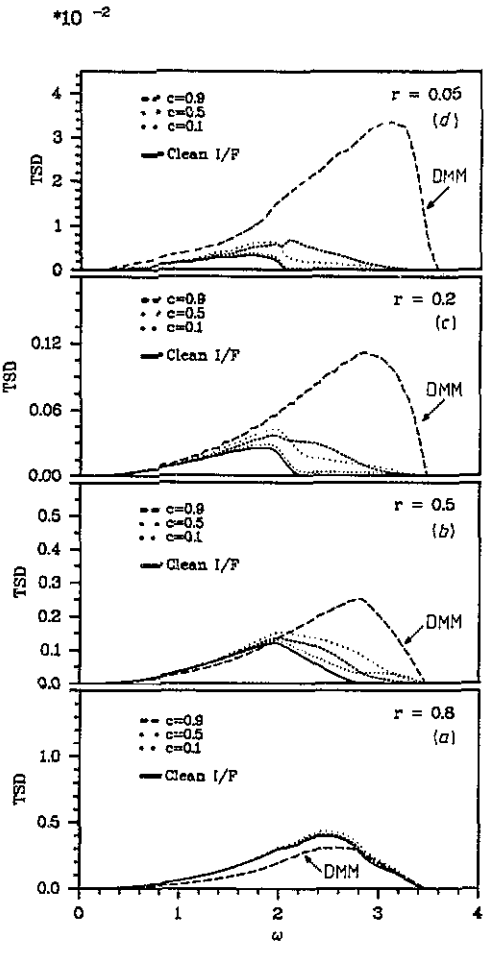

Figure 4. Comparison between DMM (indicated by an arrow), planar boundary (——) and CPA (all other lines) results for the TSD.

In what follows we have constantly assumed that $m_A = f_A = f_B = f_{AB} = 1$ and $m_B \leqslant 1$. We show in figures 3 and 4 the TSD ((16), (20)) for different mass ratio values that sample the whole range of impedance ratios for the most common metal–insulator boundaries (approximately from 1/1 up to 1/5) [6]. The degree of interface disorder has been varied through the value of the light-atom concentration in the interface alloy.

For small mismatch values (figure 3(*a*)) the diffuse phonon scattering makes only a minor contribution to the TSD near the maximum frequency of the heavy crystal; thus, specular phonon scattering and diffuse phonon scattering occur over a common frequency range. In addition, the small values of the diffuse scattering rates indicate that the VCA is a good approximation in treating the boundary alloy. Compared with the TSD for the clean boundary (figure 4(*a*)), the VCA and CPA predict an increased TSD, while the DMM predicts a decreased value. The reason for this qualitative difference lies in the basic assumption of the DMM that the phase coherence is complete lost for phonons scattered at the boundary; this is a bad approximation when the mismatch is small and

the 'critical cone' wide [15]. Finally, note that the CPA and VCA results do not change appreciably with the interface alloy composition; this behaviour is expected, because the alloy potential is weak ($\sim \Delta m\, \omega^2$).

As the mismatch grows (figures 3(*b*)–3(*d*) and 4(*b*)–4(*d*)), the role of diffuse scattering becomes increasingly important, as expected, and for certain frequencies and alloy compositions makes the dominant contribution. The maximum of the diffuse scattering appears at around the cut-off frequency for specular transmission; this feature arises because phonons at this frequency suffer total specular reflection at the boundary and therefore have a quite substantial amplitude at the disordered interface plane, which makes them particularly sensitive to the alloy fluctuations. The DMM neglects the possibility of total reflection and predicts maximum transmission near the maximum frequency of the heavy crystal, which is simply a bulk VDOS effect (see figure 4). Note also that the diffuse component of the TSD is very sensitive to the alloy composition unlike the specular component. Furthermore, the CPA again predicts an increase in the TSD compared with the clean boundary, but opposite to the case of small mismatch, with values lying below the DMM predictions. As we mentioned above, we can attribute this feature to the assumption that in the DMM it is possible for *all* phonons to transmit by escaping outside the critical cone; since for large mismatches the cone is very narrow, the transmission is greatly enhanced by this assumption. The CPA, on the other hand, also allows phonons to escape outside the critical cone, but the interference effects that are included (up to the single-site approximation) impose restrictions on the escape process. Finally, note that an asymmetry develops in the CPA results around the case of maximum disorder ($c = 0.5$) with increasing mismatch and, therefore, with inceasing values of the alloy potential. The VCA results remain symmetric. This dependence on alloy composition is similar to bulk alloy spectra [13, 14].

Consider next the results for the conductivity, equation (12), shown in figure 5. At low temperatures ($\Theta \ll 1$) it shows a power-law dependence on the temperature and at high temperatures ($\Theta \geqslant 1$) it is constant (saturation regime). The CPA treatment shows that the effect of the interface roughness is to increase the TBC at all temperatures, for any boundaries and any interface alloy composition. The same conclusion has been reached in the treatment of the problem in the continuum limit [12]. On the contrary, the DMM predicts a reduction in the conductivity for small mismatch values (figure 5(*a*)) and an increase for large mismatch values (figure 5(*d*)); a crossover is seen at intermediate mismatch (figures 5(*b*) and 5(*c*)). The origin of these differences has been discussed above, in connection with the TSD.

The temperature dependence is also modified by the interface roughness. The evaluation of the slope of the CPA curves in figure 5 has shown that for sufficiently low temperatures ($\Theta \leqslant 0.1$) the temperature exponent is increased by $\nu \leqslant 0.5$. The deviations from the T^3-law predicted by the DMM occur at higher temperatures than the microscopic model, as can be clearly seen for large mismatch values. The origin of this behaviour lies in the assumption made in the DMM that the transmission coefficient is independent of the incident phonon wavevector, equation (16); consequently, high-frequency phonons (i.e. dominant phonons at $\Theta \simeq 1$) for which the scattering cross section is highly anisotropic [13] are basically treated similarly to phonons in the linear dispersion regime that are known to give rise to the T^3-dependence [16].

Major changes due to the interface roughness occur in the saturation regime, where the dominant phonon wavelength is comparable with the defect size (about a). We show in figure 6 the dependence of the saturation conductivity, equation (14), on the mismatch and interface alloy composition. The asymmetry of the CPA results around the maximum

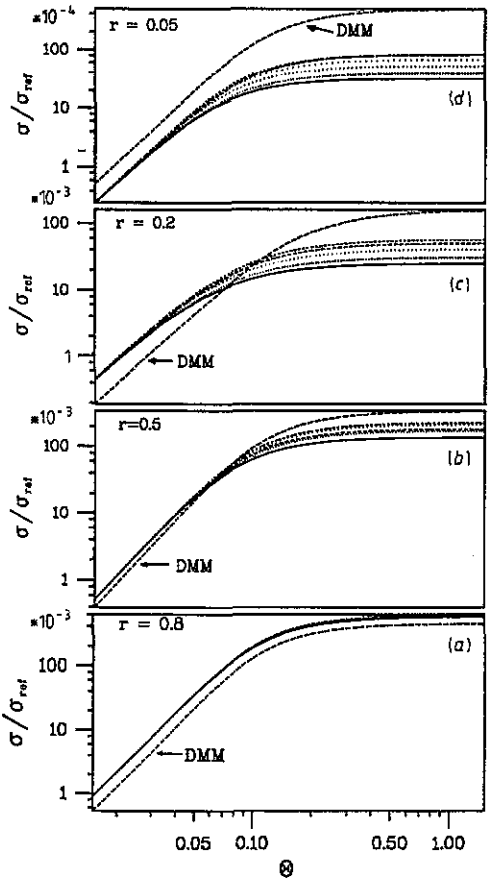

Figure 5. TBCS: ——, planar boundary; – – –, DMM; other lines, CPA for various alloy concentrations.

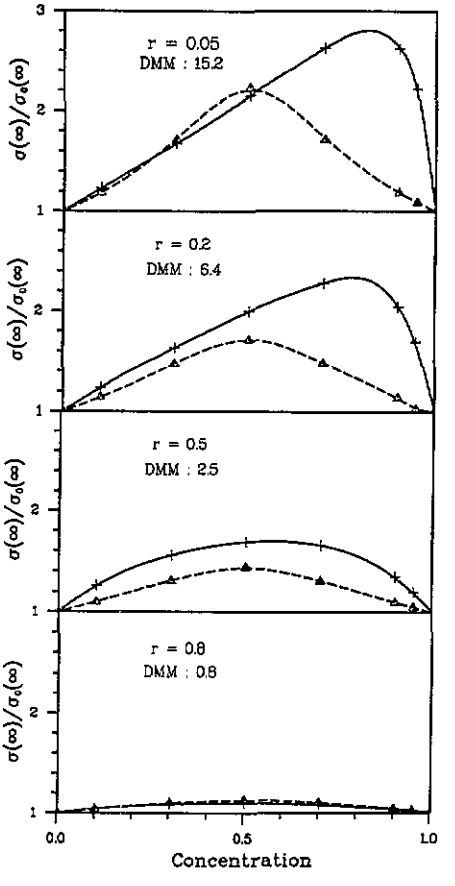

Figure 6. Saturated TBCS: ——, CPA; – – –, VCA; the markers indicate the computed points and the lines serve only as a guide to the eye.

disorder is a direct consequence of the same asymmetry appearing in the TSD. The CPA and VCA results are comparable for certain mismatch and alloy concentration values. At certain parameter values, the alloy acts as a weakly scattering medium and the fluctuations become unimportant, and the VCA and CPA results are comparable. The prediction for such a behaviour could be deduced by simply examining the imaginary part of the self-energy [14]. Note, finally, that for small mismatch values the alloy is always weakly scattering for all concentrations.

4. Conclusions

We have presented a first fully microscopic calculation of the thermal boundary conductivity between two crystals including the effect of atomic-scale roughness within a monolayer. Our results indicate an increase in the conductivity at all temperatures relative to the planar boundary. In the saturation regime the increase is by a factor of 2–3 for impedance ratios of $\frac{1}{2}$–$\frac{1}{5}$, which is of the same magnitude found in recent experiments

such as those by Young *et al* [3] and Swartz and Pohl [6]. This suggests that the interface roughness could be responsible for the discrepancies between theory and experiment. The comparison with a phenomenological model (DMM) has shown qualitative disagreement for small mismatch values, since the latter predicts a conductivity reduction due to roughness, and a rather quantitative disagreement for large mismatch values, where the DMM predicts much larger increases. The DMM is therefore expected to be of reduced validity in the high-temperature regime and nearly ideal interfaces, as, for example those grown by MBE. Future experiments in this direction would be very useful.

For a better comparison with recent experiments, certain aspects of our model should be improved and extended. For example, the use of a more realistic lattice dynamical model, the inclusion of more than one disordered layer and the comparative study of different types of defect, such as dangling bonds and islands.

Acknowledgments

I would like to thank Professor R J Elliott for useful discussions, Professor J C Inkson, Dr R T Phillips and Dr P R Briddon for their comments and Dr G P Srivastava for a critial reading of the manuscript. Financial support from the Science and Engineering Research Council is acknowledged.

References

[1] See, e.g., the reviews by
Anderson A C 1981 *Nonequilibrium Superconductivity, Phonons and Kapitza Resistance* (New York: Plenum) p 1
Wyatt A F G 1981 *Nonequilibrium Superconductivity, Plasmas and Kapitza Resistance* (New York: Plenum) p 31
Swartz E T and Pohl R O 1987 *Appl. Phys. Lett.* **51** 200
[2] Wybourne N M and Wigmore J K 1988 *Rep. Prog. Phys.* **51** 923
[3] Young D A, Thomsen C, Grahn H T, Maris H J and Tauc J 1986 *Phonon Scattering in Condensed Matter* ed A C Anderson *et al* (Berlin: Springer) p 49
Swartz E T and Pohl R O 1986 *Phonon Scattering in Condensed Matter* ed A C Anderson *et al* (Berlin: Springer) p 228
[4] Stoner R, Young D A, Maris H J, Tauc J and Grahn H T 1989 *Phonons 89* ed S Hunklinger (Singapore: World Scientific) p 1305
[5] Swartz E T and Pohl R O 1987 *Appl. Phys. Lett.* **51** 200
[6] Swartz E T and Pohl R O 1988 *Rev. Mod. Phys.* **61** 605
[7] Steinbruchel C 1976 *Z. Phys.* B **24** 923
[8] Lumpkin M E, Saslow W M and Visscher W M 1978 *Phys. Rev.* B **17** 4295
[9] Jex H 1986 *Z. Phys.* B **63** 91
[10] Streib H M and Mahler G 1987 *Z. Phys.* B **65** 483
[11] Young D A and Maris H J 1989 *Phys. Rev.* B **40** 3685
[12] Adamenko I N and Fuks I M 1970 *Sov. Phys.–JETP* **32** 1123
Haug H and Weiss K 1972 *Phys. Lett.* **40A** 19
Shen T Castiel D and Maradudin A A 1981 *J. Physique Coll.* **42** C6 819
Shiren N S 1981 *Phys. Rev. Lett.* **47** 1466
Khater A and Szeftel J 1987 *Phys. Rev.* B **35** 6749
[13] Kechrakos D 1990 *J. Phys.: Condens. Matter* **2** 2637
[14] Elliott R J, Krumhansl J and Leath P L 1974 *Rev. Mod. Phys.* **46** 465
[15] The term 'critical cone' is used here not in the classical sense, because it varies with frequency. One could think of it as an average quantity over all frequencies.
[16] The saturation in the DMM is reached through the VDOS dependence.